

NO-R191 494

FUNDAMENTAL ASPECTS OF THE STRUCTURE OF SUPERSONIC
TURBULENT BOUNDARY LAY. (U) PRINCETON UNIV NJ DEPT OF
MECHANICAL AND AEROSPACE ENGINEERIN. A J SMITS

1/1

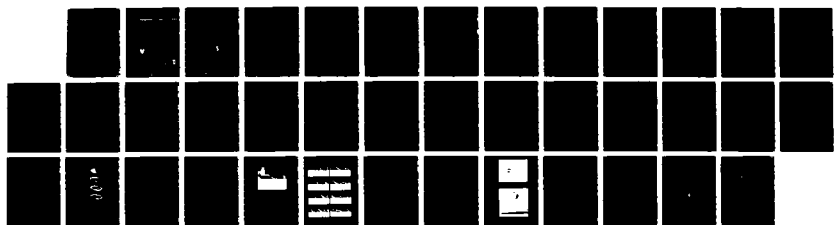
UNCLASIFIED

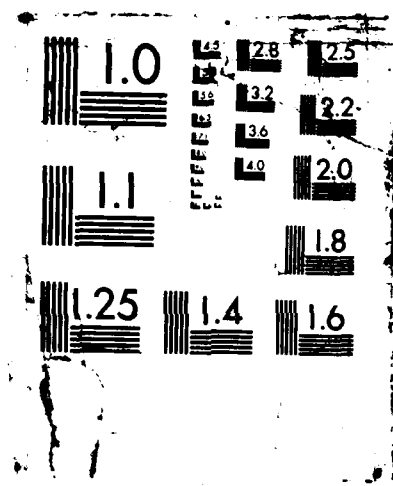
21 JAN 88 AFOSR-TR-88-0028 AFOSR-85-0126

F/G

20/4

NL





DTIC FILE COPY

(2)

AD-A191 494

AFOSR-TK- 88-0028

Princeton University

AFOSR CONTRACT 85-0126

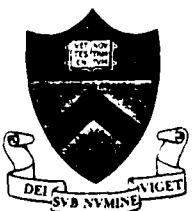
Fundamental Aspects of the Structure of
Supersonic Turbulent Boundary Layers

Contract Monitor: J. McMichael

FINAL REPORT

by

Alexander J. Smits



Department of
Mechanical and
Aerospace Engineering

DTIC
SELECTED
FEB 24 1988
S E D
C E

88 2 24 115

This document has been approved
for public release and sales by
distribution is unlimited.

2

AFOSR CONTRACT 85-0126

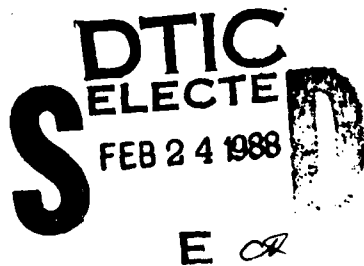
Fundamental Aspects of the Structure of
Supersonic Turbulent Boundary Layers

Contract Monitor: J. McMichael

FINAL REPORT

by

Alexander J. Smits



January , 1988

Mechanical & Aerospace Engineering Department
Princeton University
Princeton, New Jersey 08544

This document has been approved
for public release and sales by
dissemination is unlimitted

UNCLASSIFIED

SECURITY CLASSIFICATION OF THIS PAGE

REPORT DOCUMENTATION PAGE

1a. REPORT SECURITY CLASSIFICATION UNCLASSIFIED		1b. RESTRICTIVE MARKINGS	
2a. SECURITY CLASSIFICATION AUTHORITY		3. DISTRIBUTION/AVAILABILITY OF REPORT	
2b. DECLASSIFICATION/DOWNGRADING SCHEDULE		APPROVED FOR PUBLIC RELEASE DISTRIBUTION IS UNLIMITED	
4. PERFORMING ORGANIZATION REPORT NUMBER(S)		5. MONITORING ORGANIZATION REPORT NUMBER(S) AFOSR-TK-88-U028	
6a. NAME OF PERFORMING ORGANIZATION PRINCETON UNIVERSITY	6b. OFFICE SYMBOL <i>(If applicable)</i> NA	7a. NAME OF MONITORING ORGANIZATION AFOSR/NA	
7b. ADDRESS (City, State and ZIP Code) Princeton, N.J. 08544		7b. ADDRESS (City, State and ZIP Code) BUILDING 410 BOLLING AFB, DC 20332-6448	
8a. NAME OF FUNDING/SPONSORING ORGANIZATION AFOSR/NA	8b. OFFICE SYMBOL <i>(If applicable)</i> NA	9. PROCUREMENT INSTRUMENT IDENTIFICATION NUMBER AFOSR-85-0126	
10. SOURCE OF FUNDING NOS		11. TITLE (Include Security Classification) Fundamental Aspects (U) of the Structure of Supersonic Turbulent Boundary Layers	
		PROGRAM ELEMENT NO 61102F	PROJECT NO. 2307
		TASK NO. A2	WORK UNIT NO.
12. PERSONAL AUTHORIS Smits, Alexander J.		13. DATE OF REPORT (Yr. Mo. Day) 1988/1/21	
13a. TYPE OF REPORT Final		13b. TIME COVERED FROM Jan 85 TO Jan 88	15. PAGE COUNT 37
16. SUPPLEMENTARY NOTATION			
17. COSATI CODES		18. SUBJECT TERMS (Continue on reverse if necessary and identify by block numbers) Turbulent flow; supersonic boundary layers, turbulence structure, high-speed flow, curved flows Aerospace (Fluid Mechanics); Flow visualization	
19. ABSTRACT (Continue on reverse if necessary and identify by block numbers) <p>Here, we give the final report for AFOSR Contract 85-0126 "Fundamental Aspects of the Structure of Supersonic Turbulent Boundary Layers," monitored by Dr. J. McMichael. This three-year contract originally had two tasks: to investigate the structure of flat plate supersonic turbulent boundary layers (Task A), and to investigate longitudinal curvature effects in turbulent boundary layers (Task B). As a result of the work performed under these task headings, we identified a need to study the structure of simple, wall-bounded vortex loops. This investigation (Task C) commenced in the third year, and we feel that it has made a major contribution to our understanding of the ensemble-averaged structure of low and high speed turbulent boundary layers. The progress reported here is that achieved in completing these three tasks since the beginning of the Contract in January 1985.</p> <p><i>Keywords:</i></p>			
20. DISTRIBUTION/AVAILABILITY OF ABSTRACT UNCLASSIFIED/UNLIMITED <input checked="" type="checkbox"/> SAME AS RPT <input type="checkbox"/> DTIC USERS		21. ABSTRACT SECURITY CLASSIFICATION UNCLASSIFIED	
22a. NAME OF RESPONSIBLE INDIVIDUAL JAMES M MCMICHAEL		22b. TELEPHONE NUMBER <i>(Include Area Code)</i> 202-767-4935	22c. OFFICE SYMBOL AFOSR/NA

INTRODUCTION

Here, we give the final report for AFOSR Contract 85-0126 "Fundamental Aspects of the Structure of Supersonic Turbulent Boundary Layers," monitored by Dr. J. McMichael. This three-year contract originally had two tasks: to investigate the structure of flat plate supersonic turbulent boundary layers (Task A), and to investigate longitudinal curvature effects in turbulent boundary layers (Task B). As a result of the work performed under these task headings, we identified a need to study the structure of simple, wall-bounded vortex loops. This investigation (Task C) commenced in the third year, and we feel that it has made a major contribution to our understanding of the ensemble-averaged structure of low and high speed turbulent boundary layers. The progress reported here is that achieved in completing these three tasks since the beginning of the Contract in January 1985.

<u>Accession For</u>	
NTIS GRA&I	<input checked="" type="checkbox"/>
DTIC TAB	<input type="checkbox"/>
Unannounced	<input type="checkbox"/>
<u>Justification</u>	
By _____	
<u>Distribution/</u>	
<u>Availability Codes</u>	
Dist	Avail and/or
	Special
A-1	



TASK A: THE STRUCTURE OF SUPERSONIC, TURBULENT BOUNDARY LAYERS

The principal aim of this task was to develop a physical model for supersonic turbulent boundary layer structure which could be used as the basis for improved calculations of turbulent flow. The effort was specifically directed towards a better understanding of the large-scale structures, that is, the energy-containing motions in the fully turbulent region, under conditions of zero and adverse pressure gradients.

The presence of "finger-like" structures in a zero pressure gradient boundary layer was established by Spina & Smits (1987). These structures are inclined at about 45° to the flow direction, they appear to have a limited spanwise and streamwise extent, and they are convected downstream for considerable distances without losing their identity. These conclusions were based on measurements taken with multiple normal hot-wire probes, multiple wall-pressure transducers, and high-contrast schlieren photographs. The analysis used space-time correlations and conditional averaging using the single-point VITA technique.

Some interesting new results have been obtained since then.

(a) Eddy-angle measurements

Measurements of the structure angle (derived from the space-time correlation of the signals from two parallel wires) have been obtained for an adverse pressure gradient supersonic layer and a zero pressure gradient subsonic layer. In the supersonic case, the initial Reynolds number based on momentum thickness R_θ was about 82,000, the static pressure rose by a factor of 1.9 in a distance of approximately $10 \delta_0$ (δ_0 is the initial boundary layer thickness), and the Mach number decreased from 2.85 to 2.10 in the same distance (Fernando and Smits,

1987). The results are shown in Fig. 1 for two different wire separations. The results of the smaller separation wires ($\xi/\delta_0 = 0.09$) show that the incoming boundary layer structure angle is around 45° over most of the layer with a decrease in angle near the wall and an increase in angle near the outer edge of the layer. The structure angle can be seen to increase by approximately 5° through the interaction. Much the same results were obtained with the larger separation wires ($\xi/\delta_0 = 0.18$) although the structure angles are consistently higher by around 5° . These angles were calculated assuming a convection velocity equal to the mean velocity half-way between the wires. The data have recently been re-analyzed assuming a fixed (invariant with wall distance) structure convection velocity of 0.8 times the free-stream velocity. The differences in structure angles between the incoming and the adverse pressure gradient boundary layers were found to be slightly smaller and of the order of the experimental uncertainty.

For the subsonic flow, structure angles have also been derived from the space-time correlation of signals from two normal wires (i.e. the technique of Spina & Smits, 1987). The results were obtained for a flat plate, zero pressure gradient layer, and a boundary layer recovering from strong convex curvature (Alving & Smits 1986; Alving et.al. 1987). The results for the zero pressure gradient boundary layer with $R_\theta = 5700$ show that the angle lies between 40 and 50 degrees for $y/\delta_0 < 0.5$ (see Fig. 1). However, the angle increases further from the wall and reaches a value around 60° near the edge of the layer. There appears to be a consistent increase in θ following the convex curvature which may be related to the new equilibrium state observed in the Reynolds stress profiles. This may imply that several different types of events may be contributing to the space-time correlation, and that some type of conditional sampling will probably

be necessary to sort out the influence of the various types of events. Work is continuing in this area.

Two additional results have been obtained with respect to the eddy angle in supersonic flow. First, by using VITA to detect significant events on one wire, and examining the simultaneous signal from the other wire, the variance of the eddy angle can be determined. Preliminary results have shown that the two signals typically have a correlation coefficient greater than 0.95, and that the variance is of the order of 15° . Second, one wire was placed as close as possible to the wall, at $y^* \approx 60$, and another wire was traversed through the layer. This method of measuring eddy angles has been tried by others, and gives very low angles throughout the layer, of order 15° to 30° (Brown & Thomas 1977, Robinson 1986). Our measurements gave similar results. As pointed out by Spina & Smits (1987), however, the variation of convection velocity with distance from the wall makes these measurements difficult to interpret, and they appear to be of limited value. Using two wires placed a short distance apart to deduce structure angles is physically more meaningful.

(b) Conditionally Sampled Results

In our previous work, the primary basis for conditional sampling was the VITA technique, and it was applied to signals from a normal wire which measures mass-flow fluctuations $(\mu u)'$. The $(\mu u)'$ signal was converted to u' using the Strong Reynolds Analogy. The results obtained in zero pressure-gradient high-Reynolds number supersonic flows agreed well with similar results from subsonic, low Reynolds number flows. However, it is not at all clear what physical meaning can be attributed to the events detected by this technique. The interpretation is limited by the fact that VITA is a single point criterion, applied to measurements of a single component of the turbulent fluctuations. Our

current emphasis, therefore, is to improve the detection technique to the point where the detected events can be given a more complete physical interpretation.

We have already found that the VITA technique can give a distorted picture of the flow structure. The primary technique which has allowed this critical interpretation of VITA is the development of a reliable and accurate crossed-wire probe, capable of giving signals proportional to instantaneous values of u' , v' (and $u'v'$) (see Fernando, Donovan & Smits, 1987). The shear stress signal $u'v'$ is highly intermittent, with sharp excursions from the background level (see Fig. 2). This signal is extremely suitable for conditional sampling. A simple threshold criterion was used to detect the events which make the greatest contribution to shear stress (for this case the threshold = $2 \bar{u}'\bar{v}'$). These events are obviously of great practical interest. Quadrant analysis was used to classify the $u'v'$ events into four categories: I (u^+, v^+), II (u^-, v^+), III (u^-, v^-), and IV (u^+, v^-).

The results were very revealing. Typically, the ensemble-averaged events were strong, and rather simple in shape (see Fig. 3). In particular, it should be noted that the u' event is single-sided, that is, it is either positive or negative. In contrast, when VITA was applied to the u' signal (instead of thresholding on $u'v'$), the event was doubled-sided, as shown in Fig. 4. These results suggest that VITA detection is subject to ambiguity, probably caused by the superposition of two types of events which can only be separately identified by using quadrant analysis.

To explain the concept, consider two individual u events detected by the shear stress criteria, one lying in quadrant II and the other in quadrant IV of the $u-v$ plane. Both are single sided events. It is possible that VITA detects both these events as positive by checking the slope at their centers. The

ensemble average of these two events would be a two sided event. Figure 5 clarifies the concept. Depending on exactly where the VITA technique checks the slope, these events could have been picked up a negative events, giving a two sided negative event. This may explain why positive and negative VITA events are nearly mirror reflections of each other, about the velocity axis.

The quadrant analysis can be used to reveal another interesting result. The ensemble-averaged events in each quadrant (as shown, for example, in Fig. 3) plot trajectories in the $u-v$ plane. Some examples of these loci are shown in Fig. 6. These trajectories will be compared to the results of the inviscid vortex skeleton model calculations described in Task C Progress. The probability density of the shear stress in the $u-v$ plane for the upstream boundary layer is plotted for various y/δ_0 in Fig. 7. There is a definite change in the character of the probability density as y/δ_0 increases. In the lower regions of the boundary layer all the equi-probability density contours are shaped more or less like ellipses, centered around the origin of the $u-v$ plane, with the major axis lying in quadrants II and IV at an angle to the u axis. As y/δ_0 increases, the major axis rotates and aligns itself with the u axis. The centers of the equi-probability density contours show two different effects: the higher equi-probability contour centers move into quadrant IV, and the remaining contour centers move into quadrant II. This behavior of the equiprobability contours with increasing y/δ_0 does not change within the interaction. The contribution to the shear stress from each quadrant and the fractional residence time in each quadrant is shown in Figs. 8 and 9 respectively, for various x positions. It is seen that the trend in the fractional contribution to shear stress with y/δ_0 is the same at all stations. Lower in the boundary layer, contributions from quadrants II and IV are approximately the same. Higher in the boundary layer the

contribution from quadrant II is larger, even though the fractional residence time in quadrant II is smaller. This implies that the contributions to the shear stress from quadrant II consists of more intense shorter duration peaks in $u'v'$. This same conclusion can be drawn from the "Hole Analysis" suggested by Lu and Willmarth (1970), and by examining the probability density of the time spent above a certain threshold shear stress, in quadrants II and IV. At all y/δ_0 there is a finite negative contribution to the shear stress from quadrants I and III. Hence, the contributions from quadrants II and IV add up to more than the total shear stress. As can be seen, in the outer part of the boundary layer, the contribution to the shear stress from quadrant II alone can be greater than the time-averaged shear stress.

c) Conditionally-Sampled Flow Visualization

We have continued to improve our flow visualization techniques. In particular, we are continuing to refine a method of conditionally sampling schlieren images of boundary layer structure in supersonic flow. In this technique, a hot-wire probe is used to detect the presence of strong, large-scale motions by using a real-time analog of the VITA detection method. Upon detection, a light source is flashed to record a microsecond exposure schlieren image on video tape. The hot-wire output is recorded simultaneously on the same video frame, and a typical image is shown in Fig. 10. The image was recorded using a CCD camera with linear gain so that the intensity can be linearly related to density gradient, and images can be added to get an ensemble-averaged picture. The conditionally sampled nature of the images means that we record only large events which are in the plane of the wire. We hope this method will remove the spatial integration effect of schlieren images. Preliminary results were presented by Smith and Smits (1986).

We have recently made high speed (40K frames/sec) laser schlieren movies of a supersonic boundary layer which clearly show the presence of strong large scale motions convecting with the layer (Smith & Smits 1988). Figure 11 is a typical sequence of frames taken from one of these movies. It is possible to "threshold" the schlieren images so that only the very strongest structures are detected. Despite the spatial integration inherent in the schlieren technique it appears possible to produce convincing images of individual structures and their evolution.

In our current work, we are using a rake of 8 hot-wires spaced in the vertical direction, and a probe consisting of 6 hot-wires arranged in the cross-stream direction, to characterize the large-scale motions in more detail. The results are under analysis.

TASK B: LONGITUDINAL CURVATURE EFFECTS IN TURBULENT BOUNDARY LAYERS

Here, we study the distortion and relaxation of an initially self-preserving zero-pressure gradient subsonic turbulent boundary layer as it passes through a region of convex curvature (see Fig. 12). The study serves two major purposes: it provides us with measurements in a subsonic zero-pressure gradient layer which can be used for direct comparison with the corresponding measurements in the supersonic case, and it allows us to study the behavior of structural parameters subsequent to the severe distortion imposed by the convex curvature.

Task B Progress

Previously, we were concerned with achieving an acceptable level of two-dimensionality in the relaxing boundary layer, while at the same time minimizing the pressure gradients in the bend. We believe these aims were achieved, and we are satisfied with the overall flow behavior.

A full set of Reynolds stress measurements has been completed, and the results were presented at the 25th Aerospace Sciences Meeting in Reno (Alving, Watmuff and Smits 1987). The results are shown in Fig. 13. The collapse of the shear stress in the outer layer at the exit of the bend, and the subsequent recovery behavior is clearly shown. At station 11, about 120 δ downstream of the end of curvature, the recovery of the shear stress profile is obviously far from complete.

The results were obtained using dynamic calibration. The advantage of this method is that the sensitivity to both velocity components can be determined directly without the need to measure wire angles or assume heat transfer laws. In the method described by Watmuff et al. (1983), the out-put signals from a crossed-wire probe were combined to produce signals sensitive only to the streamwise and the normal velocity components respectively. This "matching" procedure was performed by adjusting analog computer circuits while the probe was subjected to velocity perturbations in the free stream by a mechanical shaker. The probe was then oscillated once more in both directions and phase-averaged values of the matched voltages were used to determine the sensitivities at a number of free-stream velocities. The final calibration was obtained by analytically integrating polynomial expressions curved-fitted to the sensitivities. Here, we have developed a new technique where the matching can be calculated from the phase-averaged values of the anemometer signals. The

sensitivities of the matched signals can be then be calculated from the original data to produce the final calibration without the need to impose further velocity perturbations. The method is considerably less time consuming than that used by Watmuff et al. since the probe does not have to be oscillated both directions twice (once for matching and then for final calibration) and it also removes any operator bias in the matching of the wires.

Our more recent focus for Task B has meant that instead of concentrating on Reynolds stress measurements for a range of curvature parameters, we have carried out measurements of structural parameters. This approach allows a more fundamental understanding of curvature effects, and provide a direct comparison with the supersonic boundary layer results. The first of these comparisons was made by measuring the structure angle in the self-preserving boundary layer upstream of curvature. The results were shown in Fig. 1, and they were discussed under Task A. Measurements have also been made using the rake of 8 hot wires described under Task A. The results are currently being analyzed and will be presented by Alving and Smits (1988).

TASK C: ANALYSIS AND CONTROL OF WALL-BOUNDED VORTEX LOOPS

It has been widely suggested that the structure of turbulent boundary layers can be described in terms of "hairpin" or "lambda"-shaped vortex loops. This physical model seems to describe equally well the dynamics of small- and large-scale motions (see, for example, Head & Bandyopadhyay, 1981, and Smith, 1984). The interpretation of our conditionally-sampled measurements has been strongly influenced by the hairpin loop model, and to aid this interpretation further we have begun to investigate the behavior of simple wall-bounded vortex loops.

At first, we tried generating these loops using the vortices shed from a hemisphere placed on the wall, similar to that used by Perry et al. (1982) and Acarlar & Smith (1984). This method proved not to be suitable for our purposes because we wished to control the frequency of generation. By controlling their formation, interactions among multiple vortex loops can be studied. The method currently in use employs a lambda-shaped wire which periodically forces laminar, vortical fluid away from the wall (see Fig. 14). The experiments were conducted in a large low-speed smoke tunnel so that combined flow-visualization and hot-wire measurements were possible.

Task C Progress

The nature of the single loops is illustrated in Figs. 15 and 16. Figure 15 shows a plan view of the loop, indicating the characteristic splaying of the legs of the vortex, and the omega-shaped head. Figure 16 shows a side view, together with signals proportional to u' and v' , as measured by the hot-wire probe visible on the left. The signals are similar to the ensemble-averaged, second-quadrant u' and v' signals shown in Fig. 3.

Simple analytical models have been developed to model these experimental vortex loops using straight-line vortex filaments. The example given in Fig. 17 shows a simple line array of five loops, and the u' and v' signals corresponding to two positions are shown in Fig. 18. The similarities to the ensemble-averaged, second- and fourth-quadrant u' and v' signals shown in Fig. 3 are obvious. The loci on the $(u' : v')$ plane for different observers are shown in Fig. 19, and there are some interesting comparisons possible with the results shown in Fig. 6.

We have continued to use the vortex loop study as support for the interpretation of our conditionally sampled measurements. We have commenced with

a study of interacting loops. We have already performed some preliminary work to examine vortex pairing by generating two different strength vortex loops down the center of the tunnel, and demonstrated that vortex pairing in wall-bounded flows is an unlikely mechanism for the growth of the attached eddies.

COMPLEMENTARY WORK

Prof. A. E. Perry has visited on two occasions, (four weeks in January 1986 and two weeks in January 1987). His suggestions and criticisms have proven to be very useful in designing our experimental work. Our current cooperation is centered on developing attached eddy models for compressible boundary layers.

In June 1986, we invited Stephen K. Robinson from NASA-Ames to visit us and discuss supersonic turbulent boundary layer behavior. Steve Robinson is one of the very few people who have approached supersonic boundary layer measurements with a view to understanding the structure of the flow (see, for example, Robinson, 1986). The visit was very constructive, and we followed up his 1986 visit with another in 1987. At that time, Robinson brought along a hot-wire rake of 8 wires which we implemented in a zero pressure gradient supersonic flow with his active cooperation. The results are being analyzed.

The meetings of the Workshop on High-Speed Boundary Layers have continued. Meetings were held to coincide with the Atlanta and Reno AIAA meetings, and a special workshop on shock-wave/boundary layer interactions was held at Penn-State in July 1987.

The list of publications produced with support of AFOSR Grant 85-0126 is given in Appendix A.

CONCLUSIONS

The work performed under this contract has succeeded on identifying and describing the large scale, coherent motions in a Mach 3 turbulent boundary layer. Both zero and adverse pressure gradient flows were investigated. A complementary study examined the relaxation ^{of} _^ a boundary layer downstream of a short region of convex curvature, in terms of the behavior of the large-scale motions. The results of both investigations have been interpreted in terms of vortex loop models of turbulent boundary layers, and have provided the preliminary basis for the development of predictive models incorporating concepts based on coherent motions.

References

Acarlar, M. S. and Smith, C. R. [1984], "An Experimental Study of Hairpin-Type Vortices as a Potential Flow Structure of Turbulent Boundary Layers," Report FM-5, Dept. of Mech. Engrg. and Mechanics, Lehigh University.

Brown, G. L., Thomas, A. S. W. [1977], "Large Structure in a Turbulent Boundary Layer," Phys. Fluids, Vol. 20.

Fernando, E.M., Donovan, J. and Smits, A. J. [1987], "The Calibration and Operation of a Constant-Temperature Crossed-Wire Probe in Supersonic Flow," to be presented at ASME Fluids Engineering Division Spring Meeting, June 1987.

Head, M. R. and Bandyopadhyay, P, [1981], "New Aspects of Turbulent Boundary Layer Structure," Journal of Fluid Mechanics, Vol. 107, p. 297.

Perry, A. E., Chong, M. S. and Lim, T. T., "The Vortex Shedding Process Behind Two-Dimensional Bluff Bodies," Journal of Fluid Mechanics, Vol. 116, p. 77.

Robinson, S. K. [1986], "Space Time Correlation Measurements for a Compressible Turbulent Boundary Layer," AIAA Paper 86-1130, AIAA/ASME 4th Fluid Mechanics, Plasma Dynamics and Lasers Conference, Atlanta, Georgia, May 1986.

Smith, C. R., [1984], "A Synthesized Model of the Near-Wall Behavior in Turbulent Behavior in Turbulent Boundary Layers," Proceedings of Eighth Symposium on Turbulence, (Ed. G. K. Patterson and J. L. Zakin), Department of Chemical Engineering, University of Missouri-Rolla.

Spina, E.F. and Smits, A.J. [1986], "Organized Structures in a Supersonic Turbulent Boundary Layer," to be presented, Ninth Australasian Fluid Mechanics Conf., Univ. of Auckland, New Zealand, Dec. 1986.

Watmuff, J. H., Perry, A. E. & Chong, M. S. [1983], "A Flying Hot-Wire System," Experiments in Fluids, Vol. 1, pp. 63-71.

Appendix A

Publications Produced Under
Sponsorship of
AFOSR Grant 85-0126

A. Published Papers

1. Baskaran, V., Smits, A.J. and Joubert, P.N., "A Turbulent Flow over a Curved Hill. Part I. Growth of an Internal Boundary Layer", Journal of Fluid Mechanics, 182: 47-83, 1987.
2. Smits, A.J. and Muck, K.C., "Experimental Study of Three Shock-Wave/Turbulent Boundary-Layer Interactions", Journal of Fluid Mechanics, 182: 291-314, 1987.
3. Fernholz, H.H., Smits, A.J. and Dussauge, J.-P., (Eds.), "A Survey of Measurements and Measuring Techniques in Rapidly Distorted Compressible Turbulent Boundary Layers," NATO-Advisory Group for Aerospace Research and Development AGARDograph, to be published 1988.
4. Smits, A.J. and Bogdonoff, S.M., "A 'Preview' of Three-Dimensional Shock-Wave/Turbulent Boundary Layer Interactions," presented at the IUTAM Symposium on Turbulent Shear Layer/Shock Wave Interactions, Palaiseau, France, September 9-12, 1985. Published by Springer Verlag, 1986.
5. Dussauge, J.-P., Muck, K.C. & Andreopoulos, J. "Properties of wall pressure fluctuations in a separated flow over a compression ramp", IUTAM Symp. on Turbulent Shear Layer/Shock Wave Interactions, Palaiseau, France, Sept. 1985. Published Springer-Verlag, 1986.
6. Spina, E.F. and Smits, A.J., "Organized Structures in a Compressible Turbulent Boundary Layer" Journal of Fluid Mechanics, 182: 85-109, 1987.
7. Andreopoulos, J. & Muck K.C., "Some new aspects of shock wave/boundary layer interactions in compression ramp flows", Journal of Fluid Mechanics, 180: 405-428, 1987.

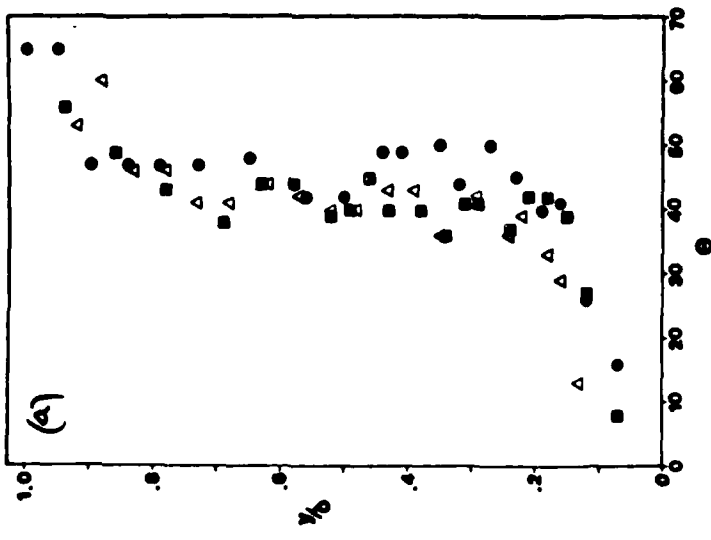
B. Papers published in Conference Proceedings

1. Alving, A.E. and Smits, A.J., "The Recovery of a Turbulent Boundary Layer from Longitudinal Curvature," AIAA Paper 86-0435, AIAA 24th Aerospace Sciences Meeting, Reno, Nevada, January 1986.
2. Andreopoulos, J. & Muck, K.C., "Some new aspects of shock wave boundary layer interactions in compression ramp flows", AIAA Paper #86-0342, AIAA 24th Aerospace Sciences Meeting, Reno, Nevada, January 1986.
3. Alving, A.E., Watmuff, J.H. and Smits, A.J., "The Relaxation of a Turbulent Boundary Layer Far Downstream of a Short Region of Convex Curvature", accepted for presentation, 25th Aerospace Sciences Meeting, Reno, Nevada, January 1987.
4. Selig, M.S., Andreopoulos, J., Muck, K.C., Dussauge, J.P. and Smits, A.J., "Simultaneous Wall-Pressure and Mass-Flow Measurements Downstream of a Shock Wave/Turbulent Boundary Layer Interaction," accepted for presentation, 25th Aerospace Sciences Meeting, Reno, Nevada, January 1987.
5. Spina, E.F. and Smits, A.J., "The Effect of Compressibility on the Large-Scale Structure of a Turbulent Boundary Layer", accepted for presentation, 25th Aerospace Sciences Meeting, Reno, Nevada, January 1987.
6. Spina, E.F. and Smits, A.J., "Organized Structures in a Supersonic, Turbulent Boundary Layer", accepted for presentation, Ninth Australasian Fluid Mechanics Conference, Univ. of Auckland, Auckland, N.Z., December 1986.
7. Fernando, E.M. and Smits, A.J., "The Effects of an Adverse Pressure Gradient on the Behavior of a Supersonic Turbulent Boundary Layer", submitted to AIAA 19th Fluid Dynamics, Plasma Dynamics and Laser Conference, Honolulu, Hawaii, September 1986.
8. Fernando, E. M., Spina, E. F., Donovan, J. F. and Smits, A. J., "Detection of Large-Scale Organized Motions in a Turbulent Boundary Layer", Proc. Sixth Symp. on Turbulent Shear Flows, Toulouse, France, Sept. 7-9, 1987, pp. 16.8.1-16.8.6.
9. Smith, M. W. and Smits, A. J., "Cinematic Visualization of Coherent Density Structures in a Supersonic Turbulent Boundary Layer", AIAA Paper 88-0500, AIAA 26th Aerospace Sciences Meeting, Reno, Nevada, January 1988.

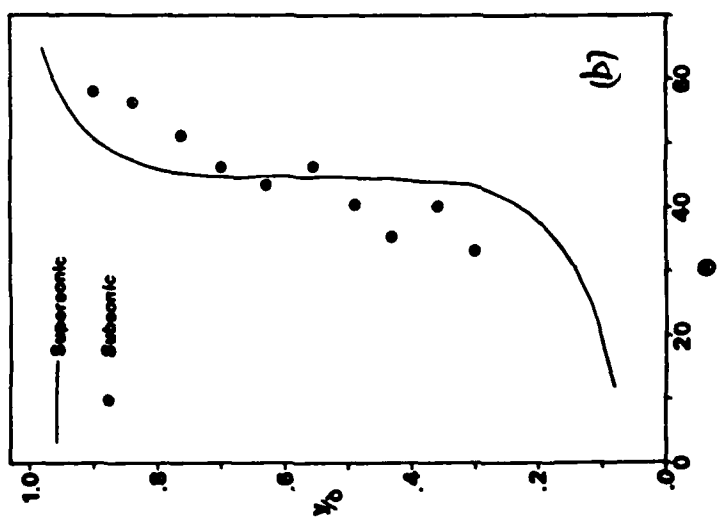
10. Alving, A. E. and Smits, A. J., "Correlation Measurements and Structure Angles in a Turbulent Boundary Layer Recovering From Convex Curvature", to be presented at the Zoran Zaric Memorial Meeting, Dubrovnik, Yugoslavia, May 16-20, 1988.
11. Fernando, E. M. and Smits, A. J., "Simple Vortex Loop Models for Supersonic Turbulent Boundary Layers", to be presented at the First National Fluid Dynamics Conference, Cincinnati, Ohio, July 24-28, 1988.
12. Smits, A. J., "Shock-Wave/Turbulent Boundary Layer Interactions: Unsteadiness and Turbulence Amplification", to be presented at the International Workshop on the Physics of Compressible Turbulent Mixing, Princeton, N. J., October 24-27, 1988.

C. Reports & Published Abstracts

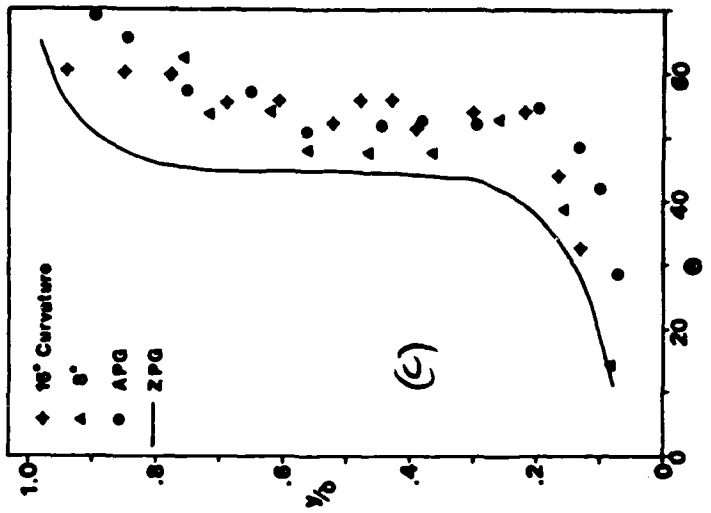
1. Rong, B.S., Tan, D.K.M. and Smits, A.J., "Calibration of the Constant-Temperature Normal Hot-Wire Anemometer in Transonic Flow", Princeton University, Dept. of Mechanical and Aerospace Engineering, Report #1696, 1985.
2. Rong, B.S., Tan, D.K.M. and Smits, A.J., "Calibration of the Constant-Temperature Inclined Hot-Wire Anemometer in Transonic Flow", Princeton University, Dept. of Mechanical and Aerospace Engineering, Report #1698, 1985.
3. Alving, A.E. and Smits, A.J., "Drag Reducing Aspects of Surface Curvature", presented at the Drag Reduction and Boundary Layer Control Symposium, Washington, D.C., Oct. 1985.
4. Spina, E.F. and Smits, A.J., "Organized Structure in a Supersonic Turbulent Boundary Layer," Paper #CPl, 38th Annual Meeting, Division of Fluid Dynamics, Bulletin of the American Physical Society, Nov. 1985.
5. Spina, E.F. and Smits, A.J., "Organized Structures in a Supersonic Turbulent Boundary Layer", Princeton University, Dept. of Mechanical and Aerospace Engineering, Report #1736, 1986.
6. Fernando, E.M. and Smits, A.J., "A Data Compilation for a Supersonic Turbulent Boundary Layer Under Conditions of an Adverse Pressure Gradient", Princeton University, Dept. of Mechanical and Aerospace Engineering, Report #1746, 1986.
7. Smith, M. and Smits, A. J., "Conditionally-Averaged Schlieren Video Images of Large-Scale Motions in Supersonic Turbulent Boundary Layers," presented, 39th Annual Meeting, Division of Fluid Dynamics, American Physical Society, Nov. 1986.
8. Donovan, J., Fernando, E. M., Selig, M. S., Spina, E. F., Watmuff, J. H. and Smits, A. J., "Active Control of Wall-Bounded Vortex Loops," presented, 39th Annual Meeting, Division of Fluid Dynamics, American Physical Society, November 1986.
9. Smith, M. W. and Smits, A. J., "A Cinematic Visualization of Coherent Density Structures in a Mach 3 Turbulent Boundary Layer", Paper #EA4, 40th Annual Meeting, Division of Fluid Dynamics, American Physical Society, November 1987.



Structure angle for different wire separations. \bullet , $4/\delta = 0.08$; \blacksquare , $4/\delta = 0.09$; \triangle , $4/\delta = 0.21$ (Spina and Smits, 1987).

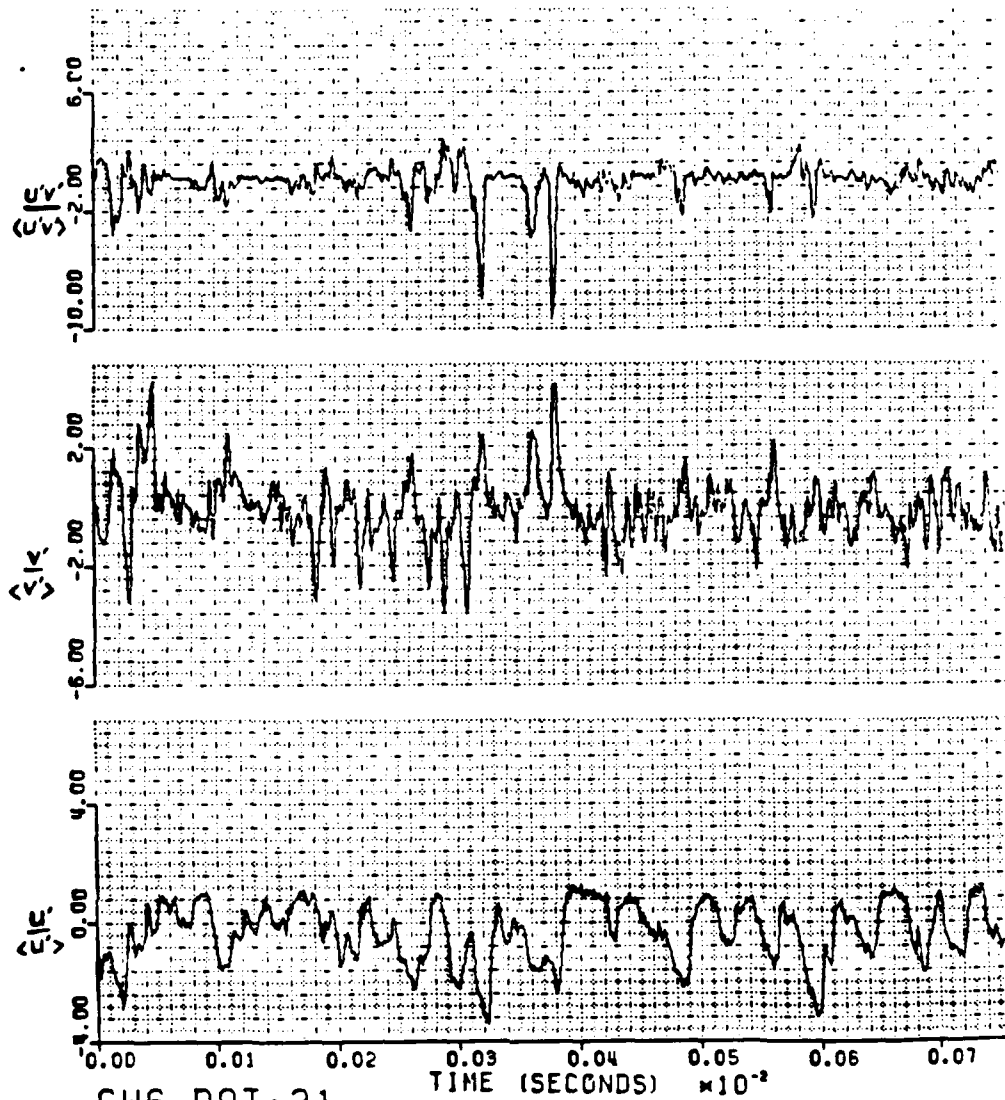


large-scale structure angle through the boundary layer as measured in subsonic flow by Alving. The supersonic distribution is a faired curve from Fig. (a)



large-scale structure angle through the boundary layer as measured in perturbed supersonic boundary layers by Fernando and Smits (1987) and Deegan and Smits (1987).

Fig. 1. Structure angle deduced from space-time correlation in zero pressure gradient subsonic and supersonic boundary layers, and an adverse pressure gradient supersonic layer.



CW6.DAT:21

LONG TIME MEAN SUBTRACTED FROM DATA & DATA NORMALIZED BY RMS OF SIGNAL
4096 POINTS FROM THE 2 TH. WRITTEN RECORD. OF THE 1TH. SAMPLED RECORD.

Fig. 2. Signals of $u'v'$, v' and u' deduced from the output of a crossed-wire in zero pressure gradient supersonic boundary layer at $y/6 = 0.65$.

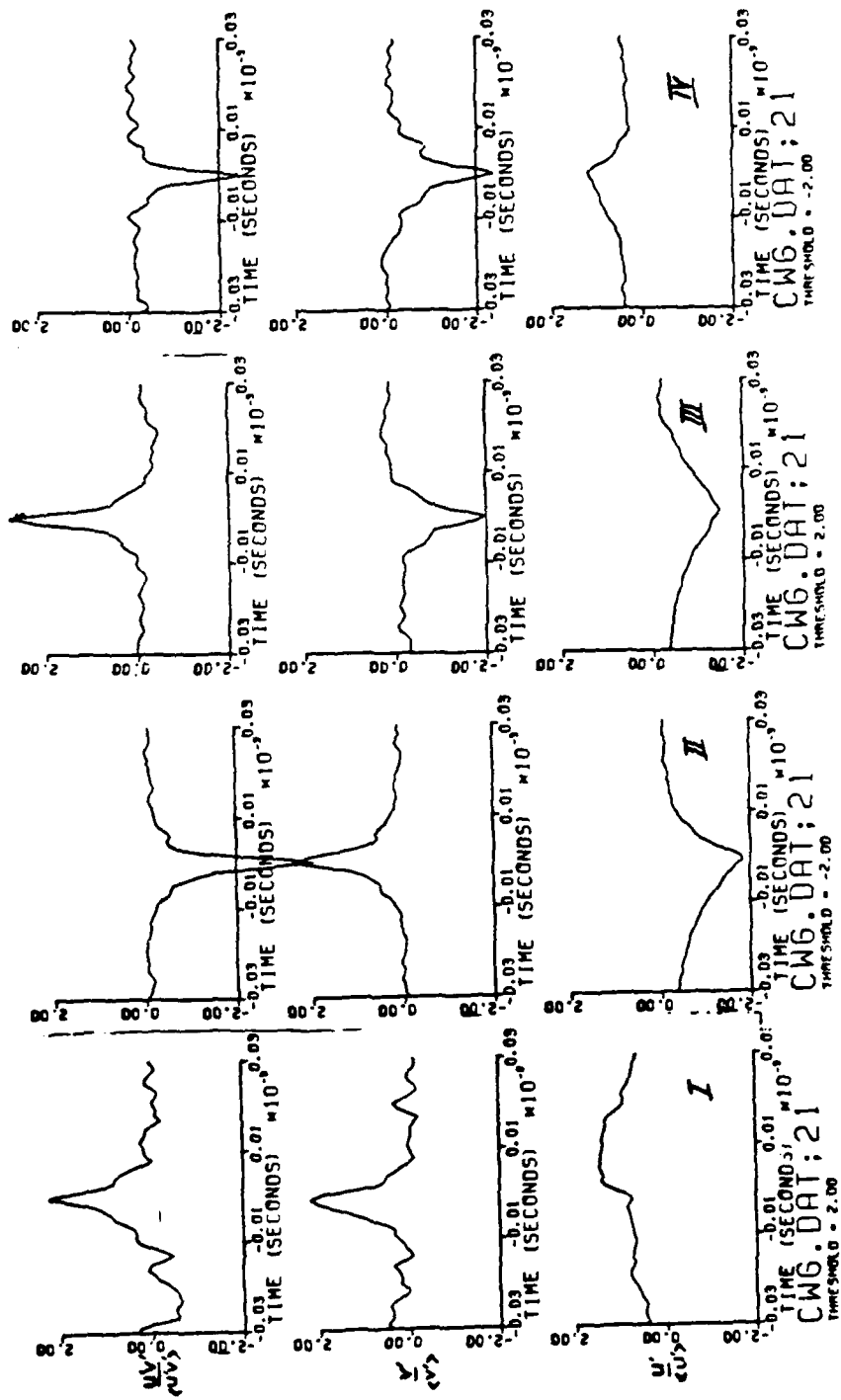


Fig. 3. Ensemble-averaged events based on threshold detection applied to $u'v'$ signal at $y/\delta = 0.65$: Quadrants I (u^+, v^+); II (u^-, v^+); III ($u^+; v^-$); IV (u^-, v^-)

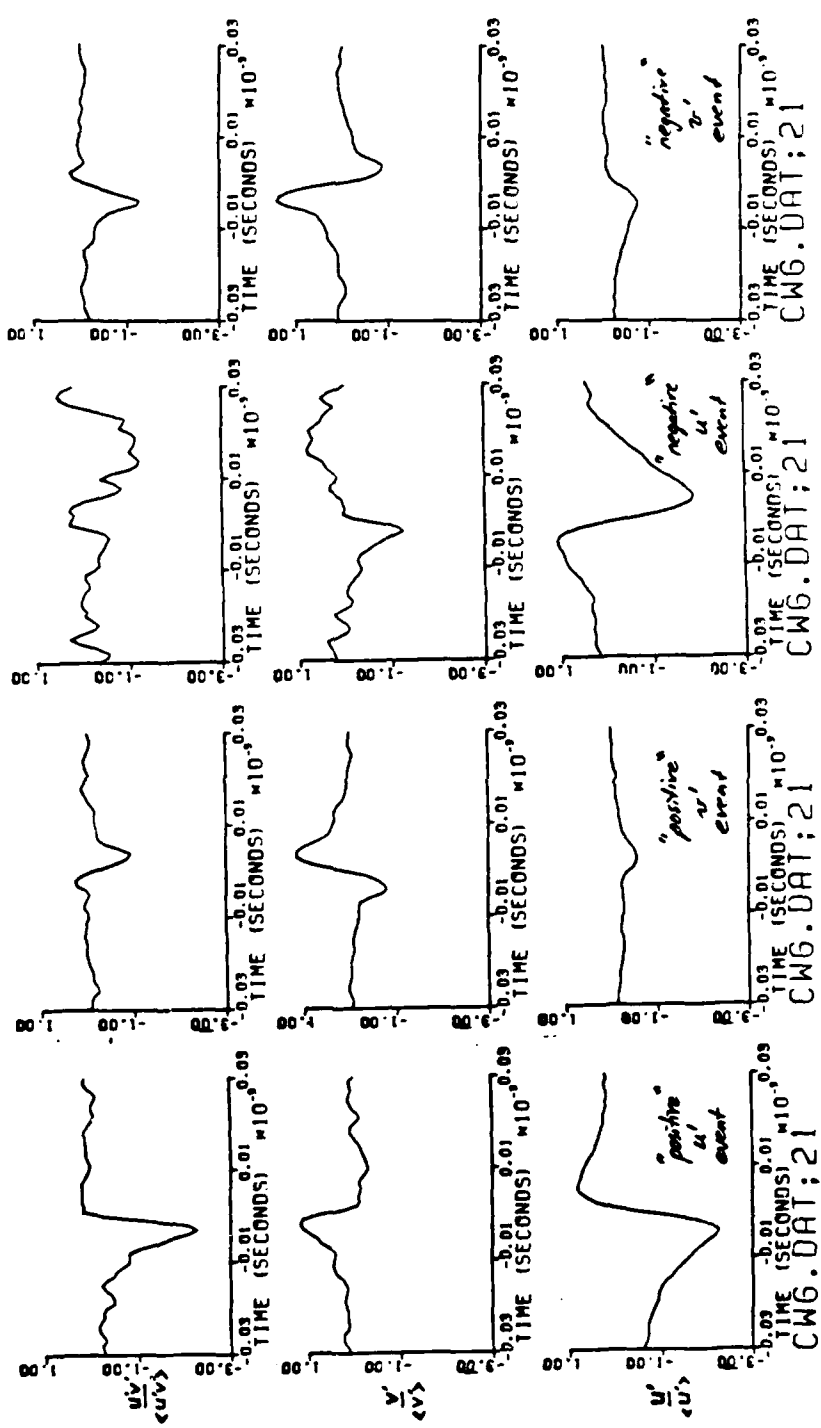


Fig. 4. Ensemble-averaged event based on VITA applied to 'u' signal
at $y/\delta = 0.65$.

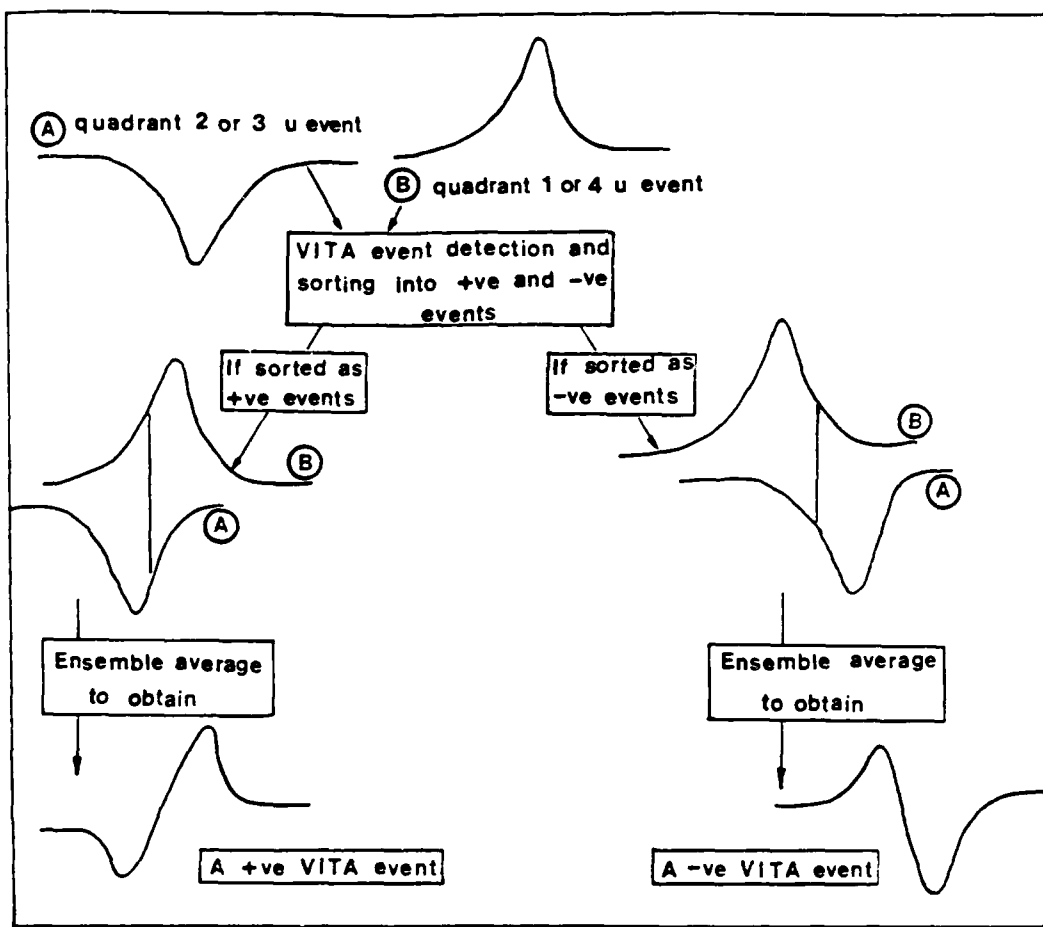


Fig. 5. Effect of sorting process on ensemble-averaged signals.

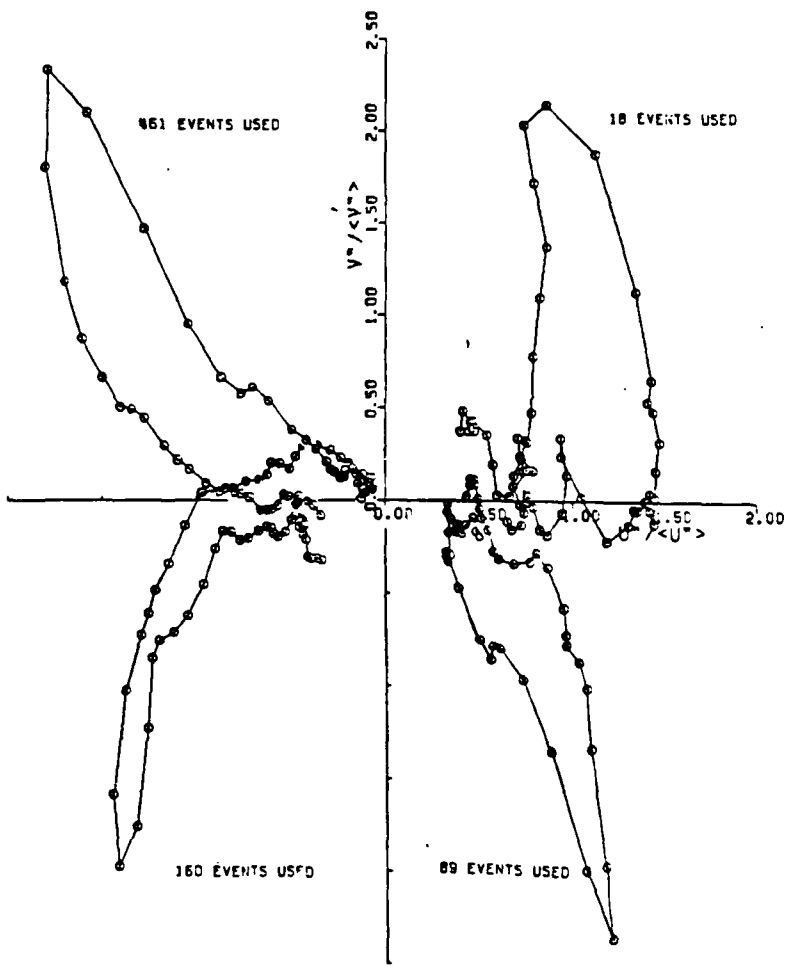


Fig. 6. Loci of the ensemble-averaged events shown in Fig. 3 in the (u' , v') plane.

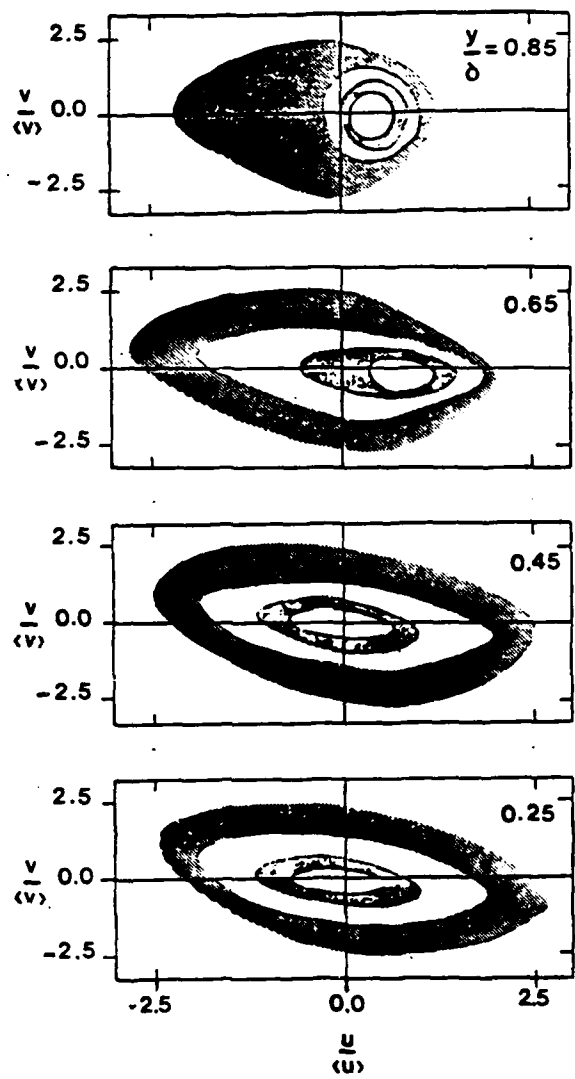


Fig. 7. Two-dimensional probability distribution of $(u': v')$ from broad-band signals.

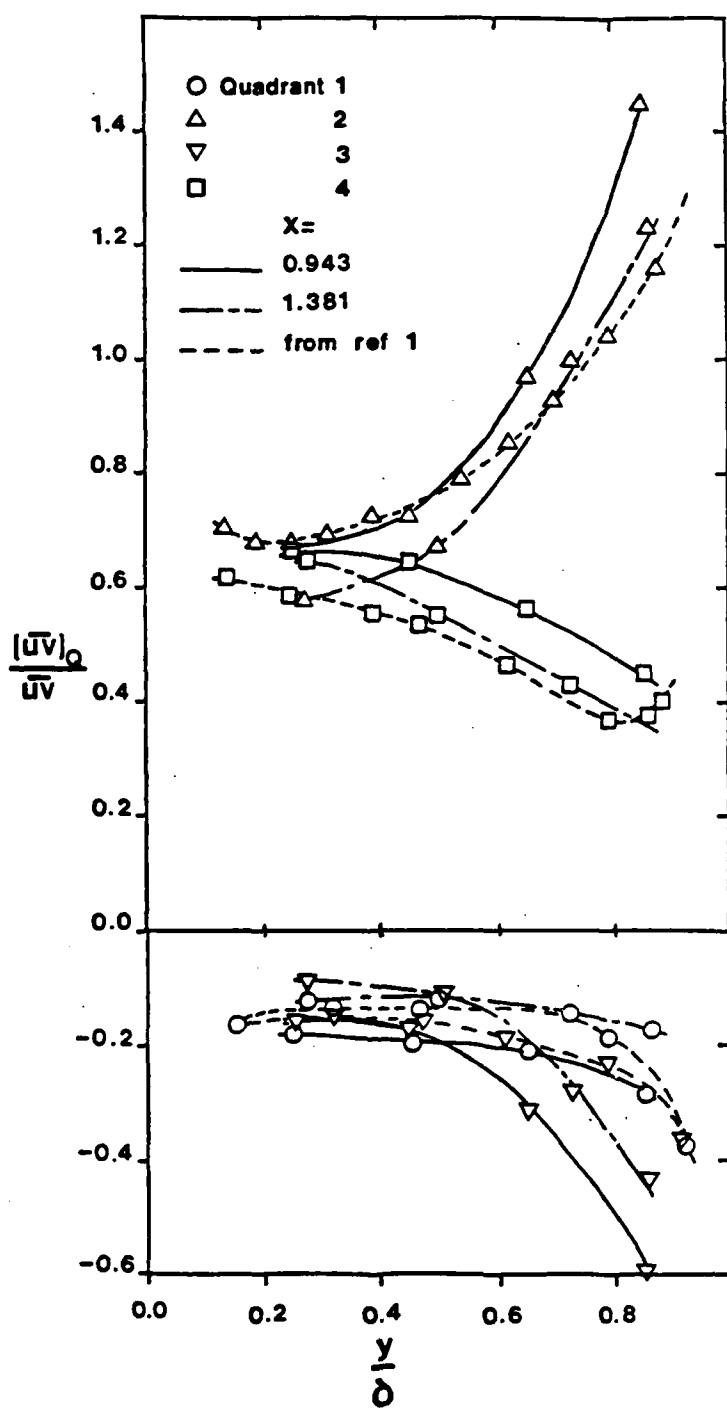


Fig. 8. Contribution to total Reynolds shear stress from each quadrant.

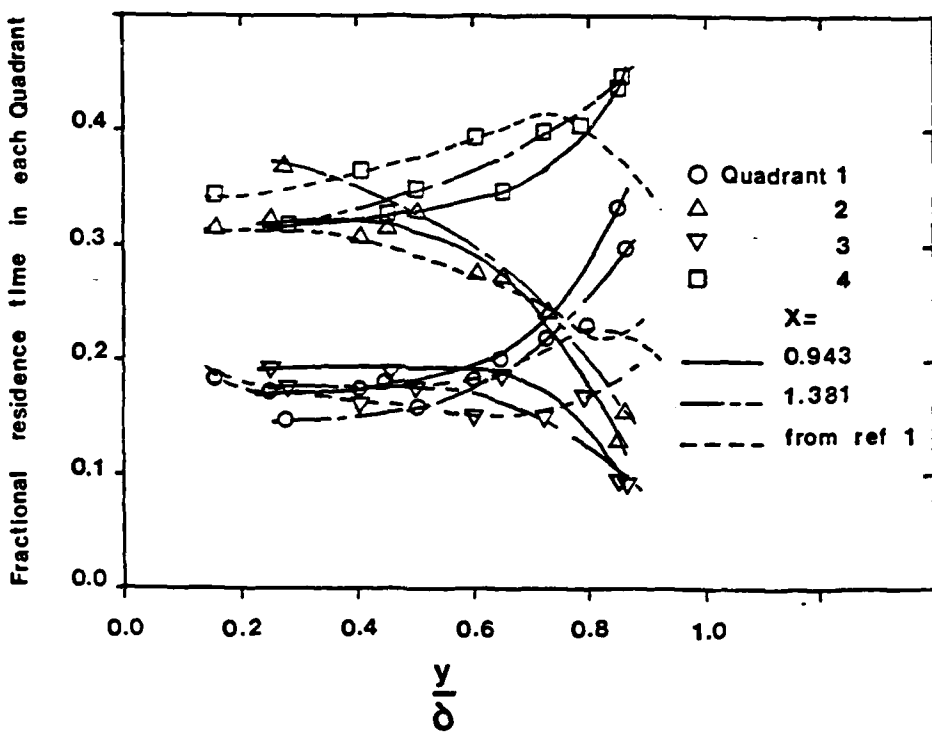


Fig. 9. Fractional residence time of Reynolds shear stress signal in each quadrant.

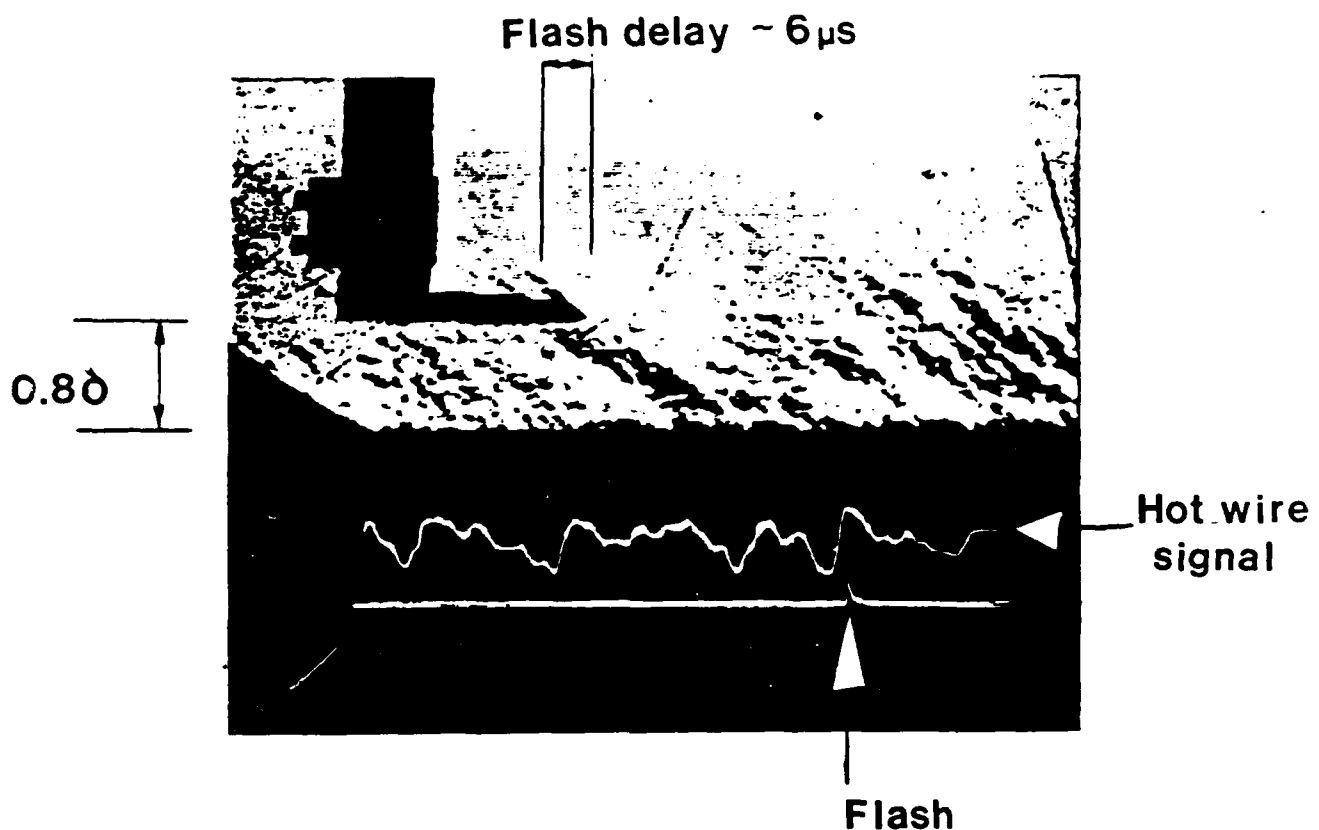


Fig. 10. Microsecond schlieren video image of zero pressure gradient supersonic boundary layer. The hot-wire probe is on the left, and the corresponding signal is shown near the bottom of the picture. The time scale corresponds approximately to the length scale of the picture.

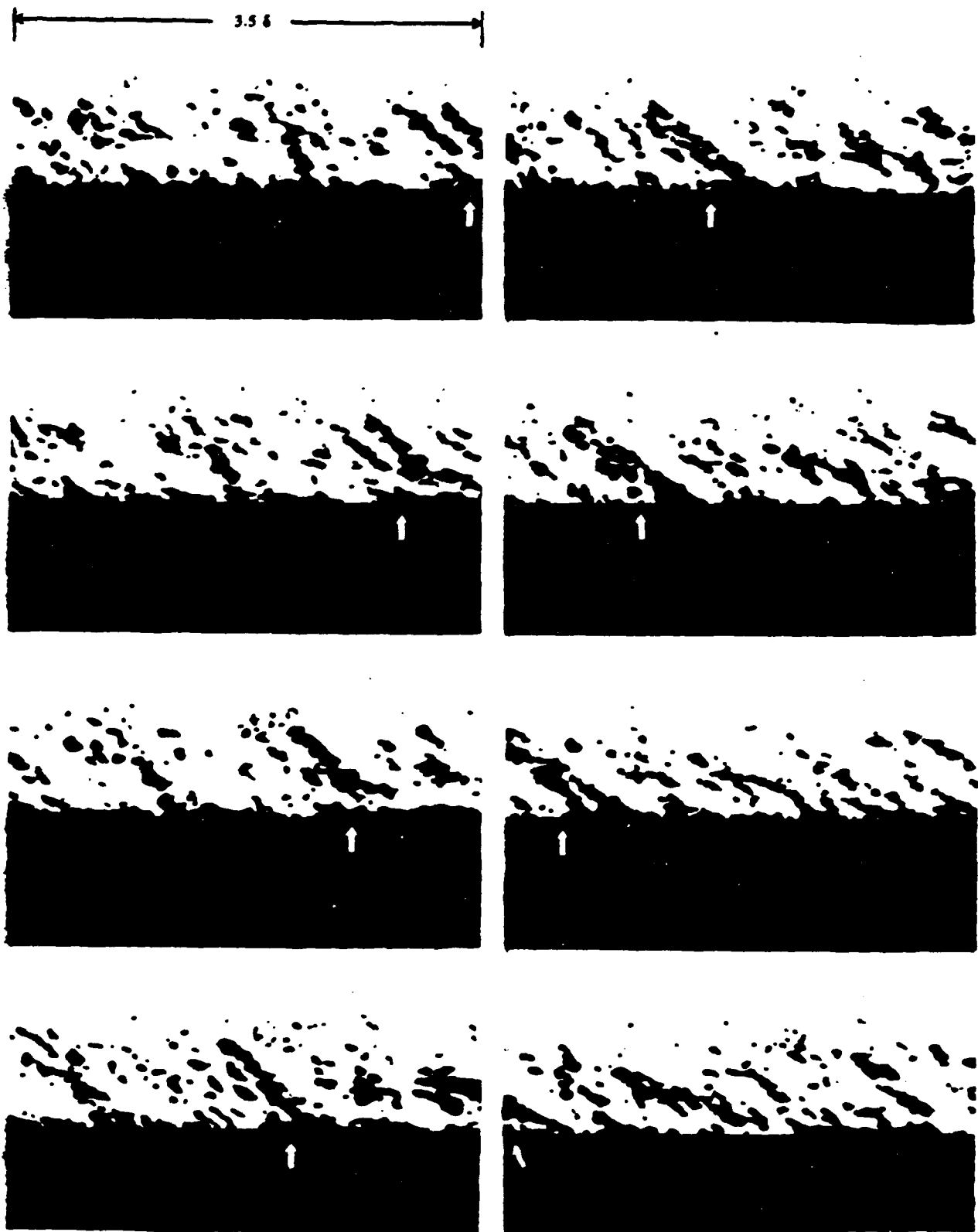


Fig. 11. High-speed laser schlieren movie of zero pressure gradient supersonic boundary layer. The images have been digitally processed to enhance the contrast. Sequence of positive events. The first frame is in the upper left, the second just below it. Flow is from right to left. Time interval between frames is approximately 27 μ secs

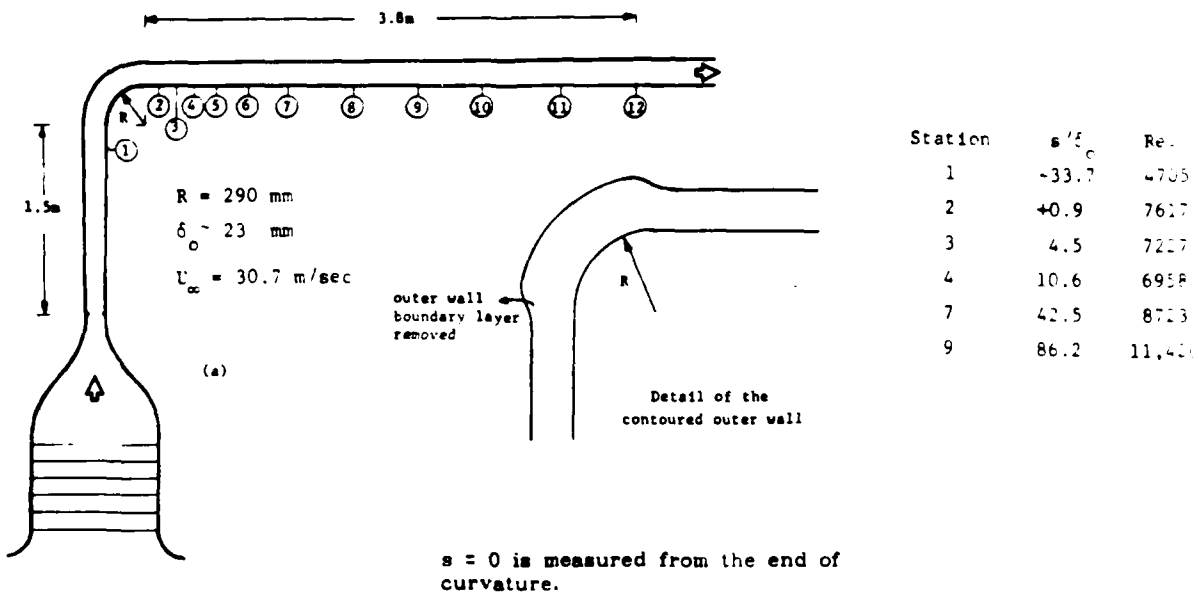


Fig. 12. Schematic of subsonic curved wall experiment, showing detail of the contoured outer wall.

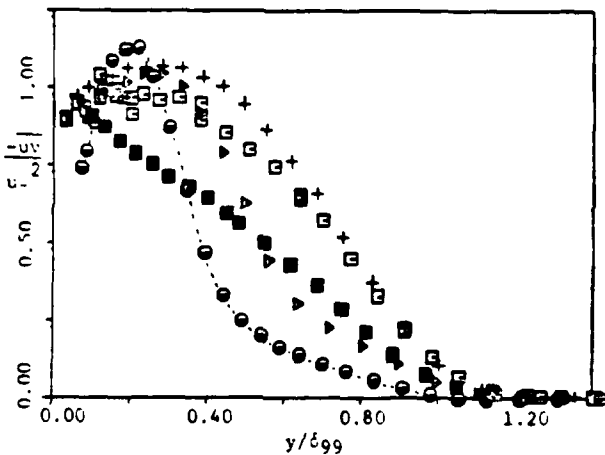


Fig. 13. Profiles of $-\bar{u}\bar{v}/u_r^2$
 ■, station 1; ○, station 3;
 △, station 5; +, station 7;
 □, station 9.

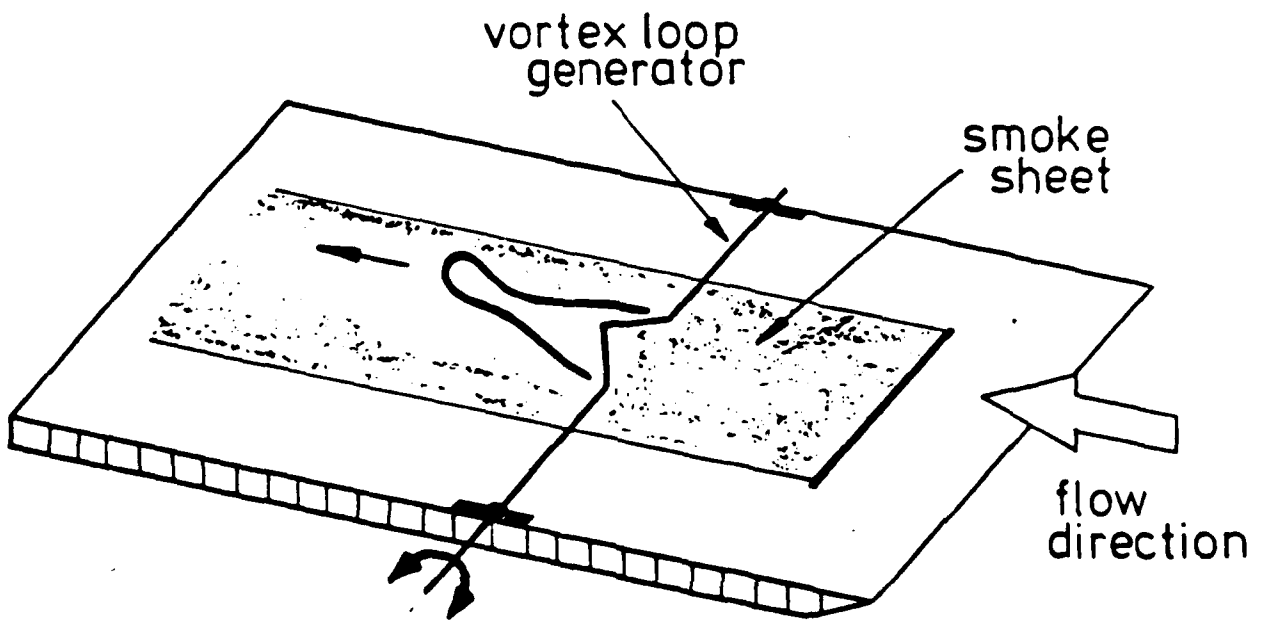


Fig. 14. Vortex loop generator.

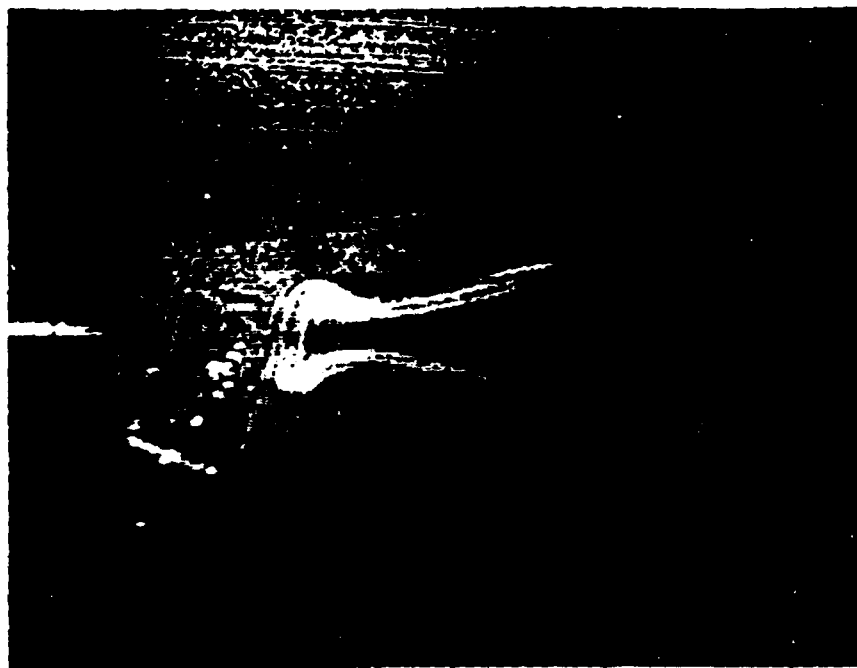


Fig. 15. Plan view of single loop. Flow is from right to left.

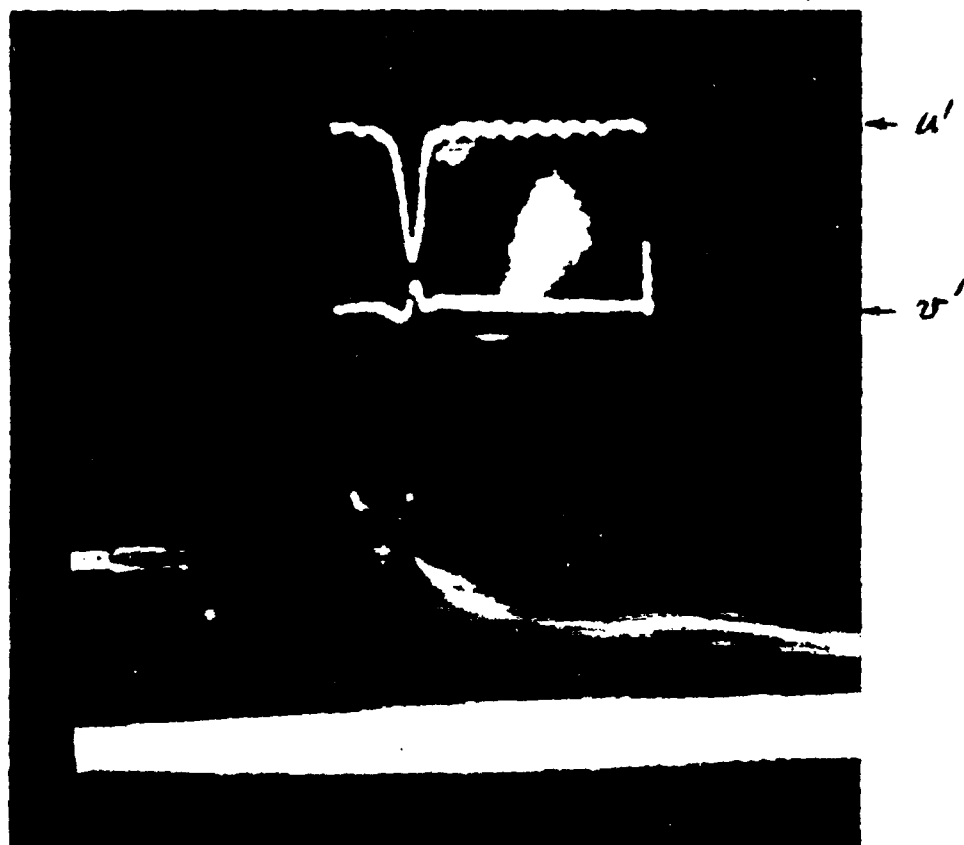


Fig. 16. Side view of single loop, showing signals recorded by hot-wire probe.

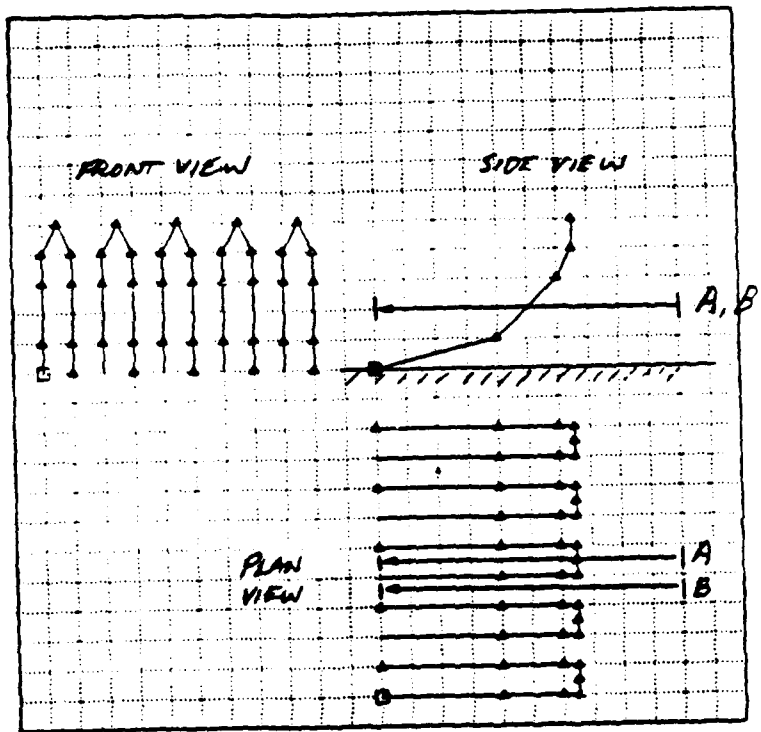


Fig. 17. Model of vortex loop array.

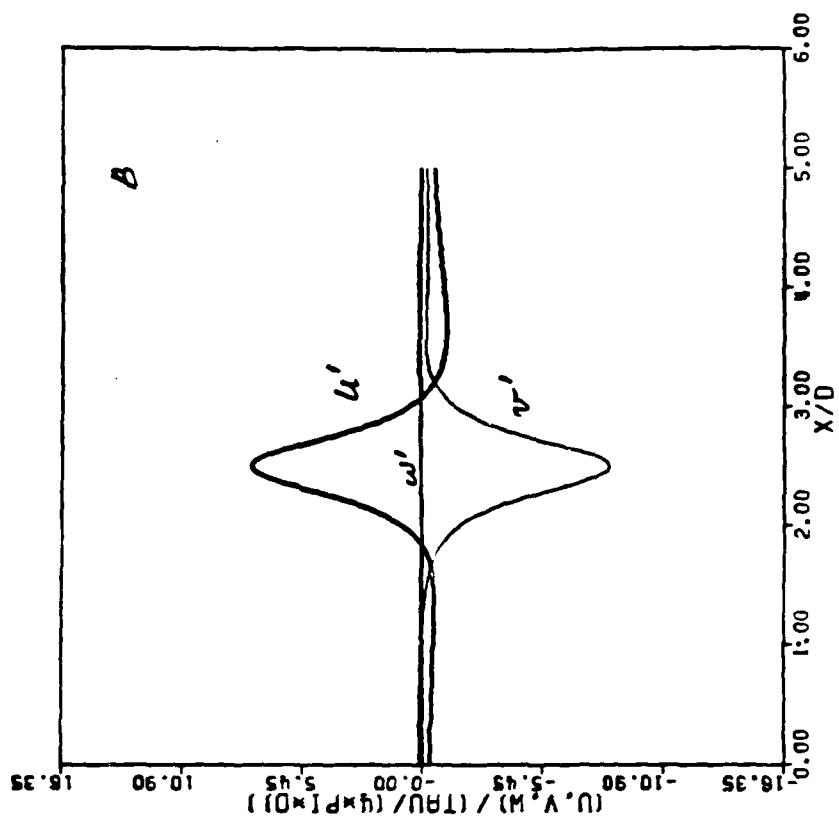
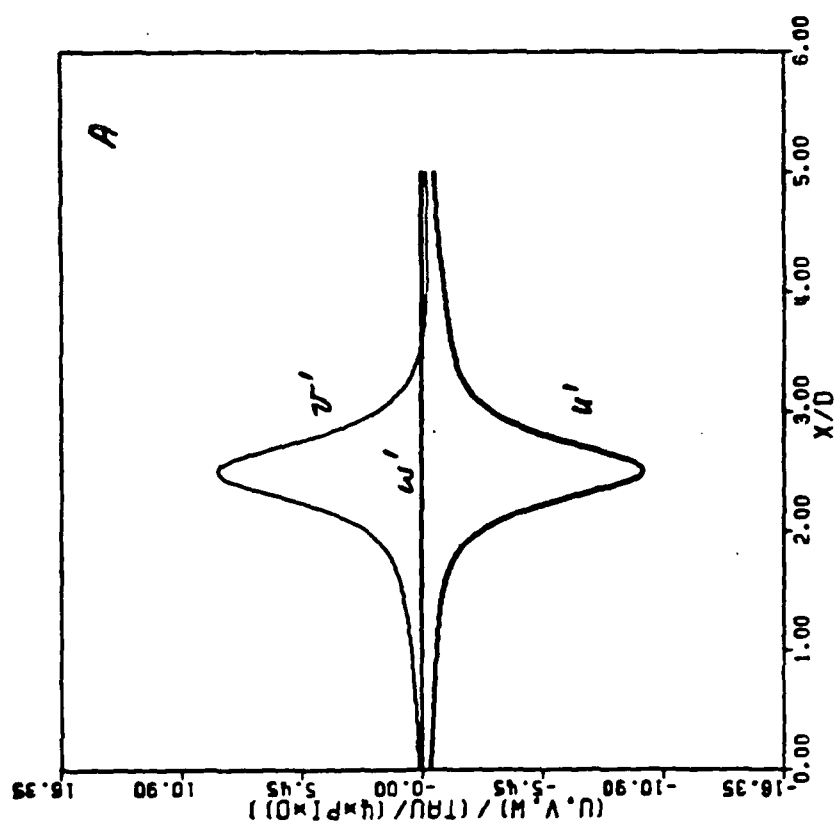


FIG. 18. Signals of u' and v' as seen by observers at A and B in FIG. 13 as the loops connect past at constant speed.

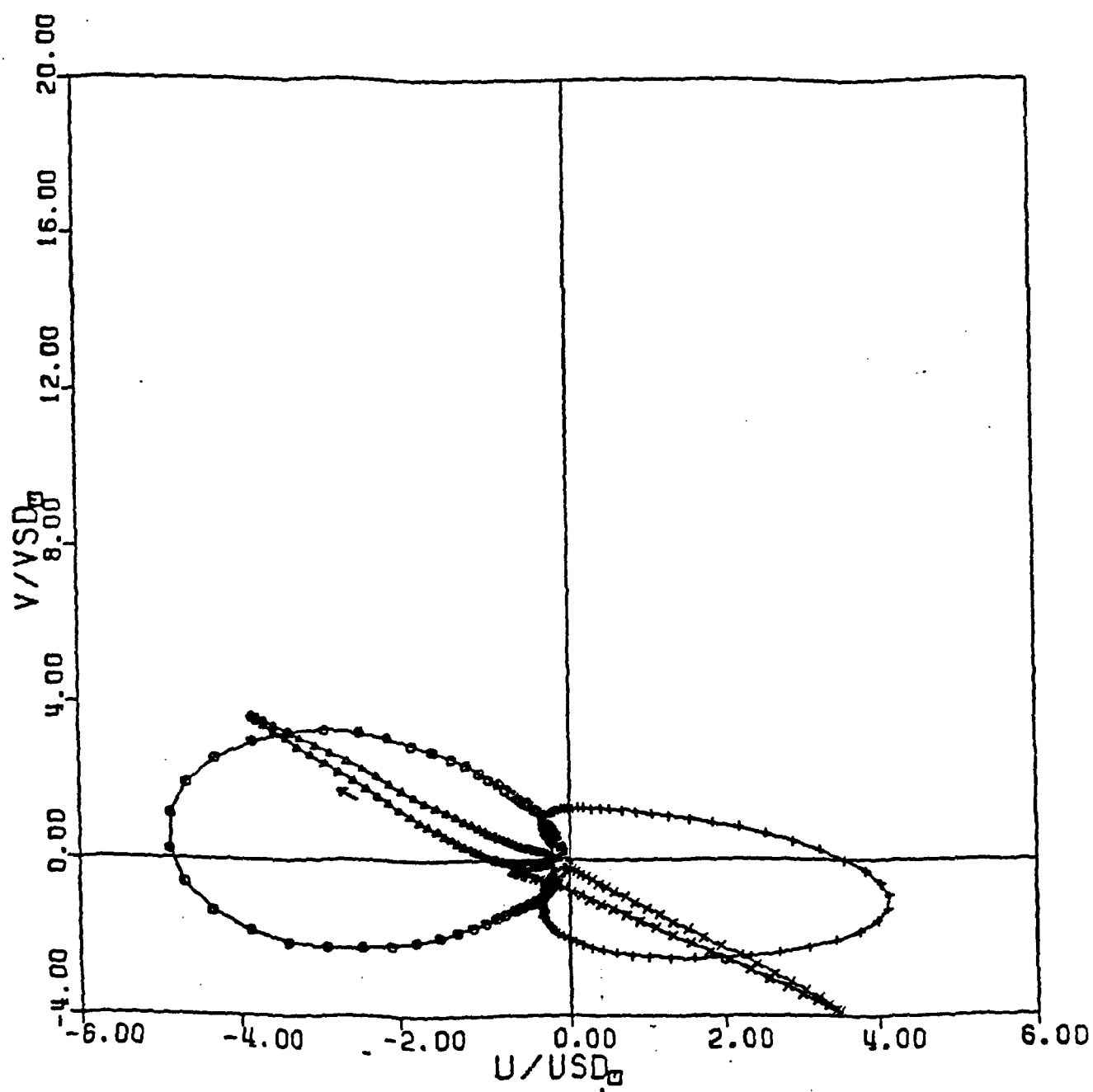


Fig. 19. Loci on the $u-v$ plane for the signals seen by observers at A and B in Fig. 17.

END
DATE

FILMED

5-88

DTIC